Futurum
Tsukuba Science Journal

Polymer/Bio Composites

Polyaniline/Bacterial Cellulose Composite

Yuki Kaitsuka, Hiromasa Goto*

Division of Materials Science, Faculty of Pure and Applied Sciences,
University of Tsukuba, Tsukuba Ibaraki 305-8573, Japan

ABSTRACT

Polyaniline (PANI) composites were prepared by oxidative polymerisation in the presence of bacterial cellulose to produce bio-material/arterial polymer composite. Chemical structure of the resultant composites was confirmed with a Fourier transform infrared spectroscopy. Thermal stability is improved through formation of composite. The carbons from composites display filament structure under the scanning electron microscopy observations.

Keywords: biomaterial; cellulose; conductivity; polymerisation

Introduction

Conjugated polymers have been paid much attention because of many possibilities for applications such as organic electronic wires, EL displays, solar cells, and anti-corrosion agent [1,2]. Among them, PANI has been widely studied such as polymerisation mechanism and reversible change in electrical conductivity in the redox (doping/dedoping) process [3-7]. Development of PANI composite has been focused on improving workability and performance for applications [8-11]. Furthermore, carbonsisation of PANI has been carried out to obtain characteristic nano or micro-structure carbons [12,13].

In this research, conductive polymer composites consisting of polyaniline and bacterial cellulose are synthesised. Bacterial cellulose as a natural nano-fibre is produced by a bacteria. Recently, high strength, transparency, and softness of bacterial cellulose have been studied [14-17]. These properties are applied for display technology and bio-functional materials [18-21]. However, there are few reports concerning PANI/bacterial cellulose composite [22-24]. We synthesised PANI/bacterial cellulose composite. Surface structure of the composites is observed with the scanning electron microscopy (SEM). Polymerisation mechanism of aniline on the surface of bacterial cellulose is discussed. Next, carbonisation of the composite is carried out to obtain carbons with unique surface structure.

Although PANI forms nano-fibers an appropriate condition in the synthesis, the resultant PANI nano-fiber length is not so much long. While, bacterial cellulose forms long fibers. Deposition of PANI on the bacterial cellulose as a substrate produces long natural textile like fibres. Based on this consideration, we carry out synthesis of PANI on the bacterial cellulose to obtain long textile like PANI nano-fibres. Furthermore, carbonization of PANI/bacterial cellulose composite provides carbon-nanofibre from the PANI composite precursor.

Received: 10 September, 2016. Accepted: 24 December, 2016
*E-mail: gotoh@ims.tsukuba.ac.jp

Experimental

Synthesis

Aniline as a monomer, (+)-10-camphorsulfonic acid (or sulfuric acid) and 0.05 wt% bacterial cellulose (nata de coco) dispersion were stirred in a vial (the quantities are listed in Table 1). The mixture was cooled to 0 °C and stirred for 1 h. Then, ammonium peroxodisulfate (APS) dissolved in minimal amount of water was slowly dropped into the mixture. After reaction for 24 h, the dark green precipitate was washed with a large volume of water, and methanol followed by filtration. The cake like product on the filter was collected and dried under vacuum to afford a desired product. We also conducted preparation of pure PANI with the typical preparation method as a reference material. Composites and polymers are abbreviated as Comp1 (PANI/cellulose prepared with APS and (+)-CSA), Comp2 (PANI/cellulose prepared with APS and H_2SO_4), Poly1 (pure PANI APS and (+)-CSA), and Poly2 (pure PANI prepared with H_2SO_4).

Table 1. Preparation of PANI/bacterial cellulose, PANI/(+)-CSA, and PANI/H_2SO_4.

Product	Aniline (mg, mmol)[a]	Acid (mg, mmol)[a]	APS (mg, mmol)[a]	0.05wt% BC[b] dispersion (mL)	Product (mg)
Comp1	51.8, 0.556	(+)-CSA (623.5, 2.684)	247.4, 1.084	5.00	15.5
Comp2	54.2, 0.581	H_2SO_4 (276.8, 2.681)	244.8, 1.072	5.00	9.7
Poly1[c]	100.9, 1.083	(+)-CSA (1246.7, 5.366)	488.3, 2.139	–	–
Poly2[c]	104.3, 1.119	H_2SO_4 (557.2, 5.397)	489.7, 2.145	–	–

[a]Sample weight and mole amount.
[b]Bacterial cellulose
[c]Distilled water is employed instead of BC dispersion

Results and Discussion

IR

Infrared (IR) absorption spectroscopy measurements with the KBr method were carried out for bacterial cellulose, Poly1, Poly2, Comp1, and Comp2 to confirm their chemical structures (Figure 1). Absorption bands derived from bacterial cellulose are observed at 3377 cm^{-1} (O-H stretching), and 616 cm^{-1} (CH out-of-plane) [24,26].

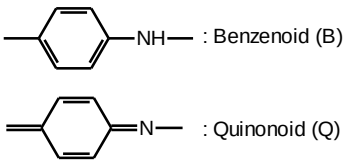

Furthermore, both composites showed typical absorption bands attributed to chemical structure of polyaniline at 3443 cm-1 (N-H stretching), 1568 cm^{-1} (quinonoid (Q) C=C stretching), 1491 cm^{-1} (benzenoid (B) C=C stretching), 1302 cm^{-1} (νQBQ C-N stretching), 1243 cm^{-1} (νBBB C-N stretching), and 1142 cm^{-1} (νQBQ C=N stretching) [9]. Here, PANI is consisting of benzenoid (B) and quinonoid (Q) units. Some absorption bands at 1568 cm-1 (νQ), 1491 cm^{-1} (νB), and 1142 cm^{-1} (νQBQ) are shifted compared with that of pure PANI (poly1 and poly2) due to interaction between polyaniline and bacterial cellulose. This result confirms formation of polyaniline/bacterial cellulose.

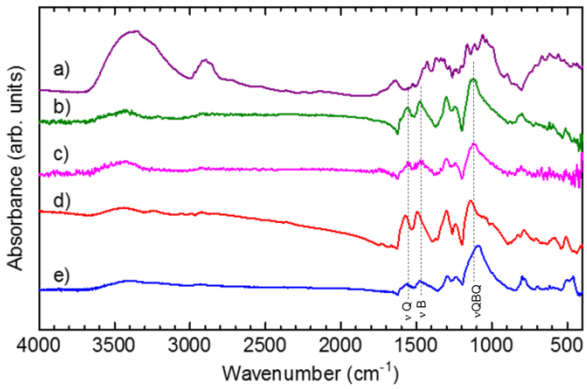

Figure 1. Fourier transform infrared (FTIR) spectra of bacterial cellulose (a), poly1 (b), poly2 (c), comp1(d), and (e) comp2.

Optical property

UV-vis absorption spectra of comp1, comp2,

poly1, and poly2 in *N*-methyl-2-pyrrolidone (NMP) were recorded (Figure 2). Absorption bands appear at 327 nm and 634 nm due to π–π* transition of benzenoid and quinonoid segments of the main-chain of PANI [25]. The signal intensity of the composites was weak compared with that of the pure PANI.

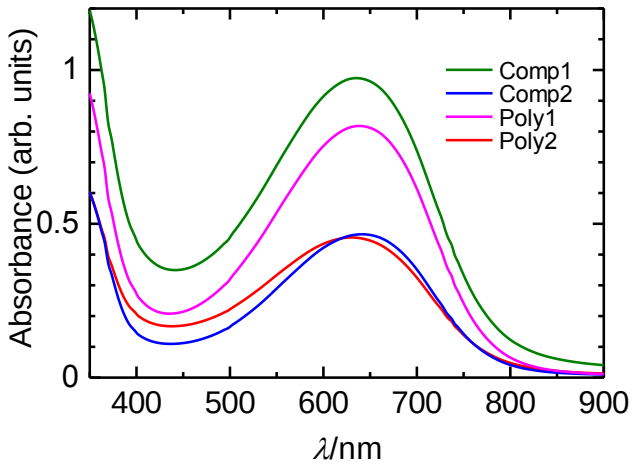

Figure 2. Ultraviolet-visible absorption spectra of comp1, comp2, poly1, and poly2 (3.75×10^{-2} [mg/mL] / NMP). NMP = *N*-methyl-2-pyrrolidone.

Morphology

Scanning electron microscopy (SEM) images of surface of comp1 and poly1 are shown in Figure 3. The pure PANI shows granular structure (Figure 3 (b)) [9]. Furthermore, partly deposition of PANI on bacterial cellulose fibre can be observed [23,24].

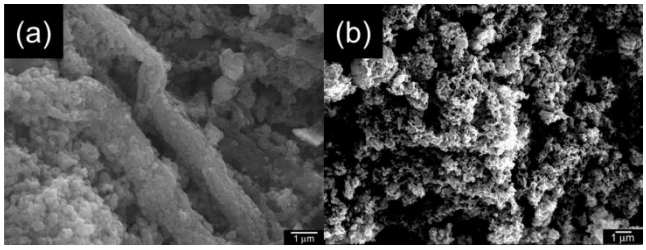

Figure 3. Scanning electron microscope (SEM) images of comp1 (a), and poly1 (b).

Electrochemical property

ESR spectroscopy measurements of poly1, poly2, comp1, and comp2 were carried out (Figure 4). All spectra indicate distribution of radicals as charge careers polarons (radical cations, Figure 4(top)) in the polymers. The g-value, line with (ΔH_{pp}), spin concentration and electrical conductivity of the samples are summarised in Table 2. In this research, g-values of the composite samples show different values from the both standard values of free electron (Table 2) [27]. A narrow peak-to-peak line width means high mobility of polarons as charge carriers [28], indicating good delocalization of polarons along the main-chain in the composite. From the ESR results, ΔH_{pp} value of the composites slightly smaller than that of the pure PANI. The main-chain of the PANI in the composite can form linearly due to interaction between PANI and bacterial cellulose. This can be comparable with concept of secondary doping of PANI in *m*-cresol [29]. However, electrical conduction between individual main-chains of PANI is suppressed due to the insulative component of the bacterial cellulose in the composite.

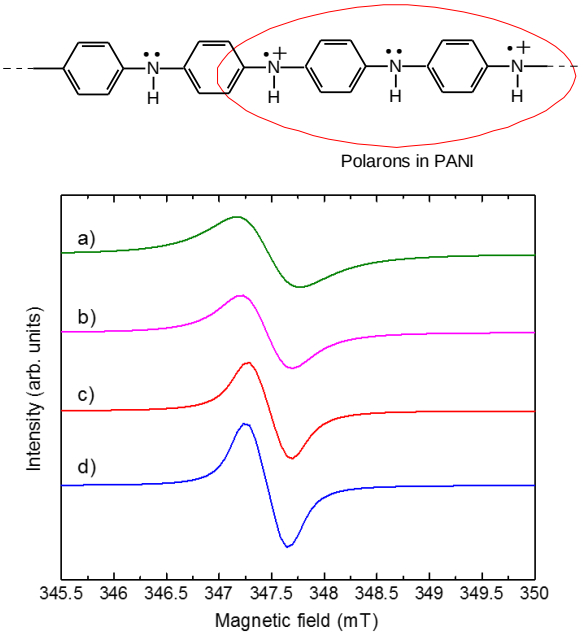

Figure 4. (Top): Polarons in PANI. Electron spin resonance (ESR) spectra of poly1 (a), poly2 (b), comp1 (c), and comp2 (d).

Table 2. ESR results and electrical conductivity.

Entry	g-value	ΔH_{pp} [mT]	*N*s [spins/g]	σ [S/cm]
Poly1	2.00386	0.586	1.16×10^{20}	0.81
Poly2	2.00331	0.469	1.36×10^{20}	3.52
Comp1	2.00358	0.410	8.11×10^{19}	2.29×10^{-4}
Comp2	2.00391	0.410	8.97×10^{19}	1.18×10^{-3}

Thermal property

The thermal behavior of Comp1, Comp2, bacterial cellulose, and poly1 was investigated with thermogravimetric analysis (TGA). The results are shown in Figure 5. Release of residual water from the sample surface occurs at 50-110 °C, and thereafter a plateau appears up to ca. 170 °C. The eight loss occurred between 170 and 280 °C with an exothermic peak probably derived from the discharge of the dopant. In the temperature range of 330-660 °C, a large mass loss of the sample was occurred. This can be explained by degradation of the PANI backbone [23,24]. The degradation of bacterial cellulose was occurred in the temperature range of 270-375 °C. Furthermore, the weight-loss of composites is lesser than that of pure PANI due to the hydrogen bond between PANI and bacterial cellulose, indicating increase of thermal stability with formation of composite.

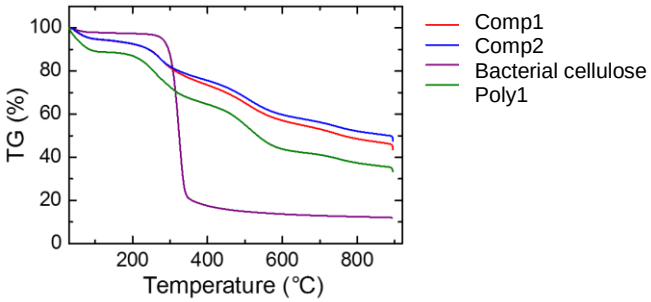

Figure 5. TGA curves of comp1, comp2, bacterial cellulose, and poly1.

Morphology after carbonisation

Carbonisation of composite was conducted at 900 °C under Ar gas flow. The SEM images of the resultant carbons from the composites are shown in Figure 6. Composites displays granular structure, however some parts of them remains cellulose nanofibre form. This fibre-shaped carbon is originated from polyaniline depositing on bacterial cellulose.

Conclusions

PANI composite was synthesised by chemical oxidative polymerisation in the presence of bacterial cellulose. The ESR measurements confirm distribution of charge carrier polarons. TG analysis indicates the composite improves thermal stability due to interaction between PANI and bacterial cellulose. The SEM observations evaluated carbonisation.

Techniques

Infrared (IR) absorption spectra for the polymers were obtained using a Thermo Scientific NICOLET iS5 with the KBr method. Ultra visible (UV-vis) spectroscopy was carried out by a JASCO V-630 spectrophotometer. Scanning electron microscopy (SEM) observations performed with a JEOL JSM-7000F. The surfaces of bacterial cellulose and composites were coated with gold with a JEOL JFC-1500 by Au sputtering. Electron spin resonance (ESR) measurements were recorded on a Bruker EMX-T ESR spectrometer. Electrical conductivity was measured by four-probe method using Mitsubishi Chemical Analytech LORESTA-GP MCP-T610. Thermogravimetric analysis (TGA) was performed on a Seiko EXSTAR7000.

Acknowledgements

This work was supported by Chemical Analysis Division Research Facility Center for Science and

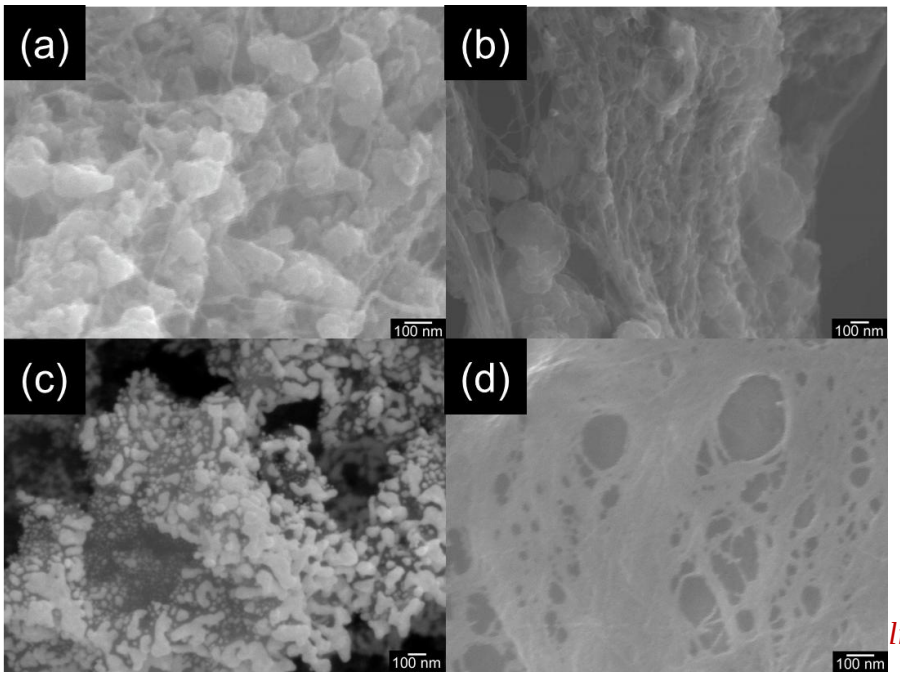

line composites

Figure 6. SEM images of carbonised comp1 (a), carbonised comp2 (b), carbonised poly2 (c), and carbonised bacterial cellulose (d).

Technology of University of Tsukuba for ESR measurements and TGA. IR measurements were carried out in Kijima laboratory of University of Tsukuba. SEM images were obtained in National Institute for Materials Science (NIMS) microstructural characterization platform.

References

1. A.G. MacDiarmid, "Synth. Met." A novel role for organic polymers (Nobel lecture), Angew. Chem. Int. Ed. Engl., 40, 2581-2590 (2001).
2. R.H. Friend, R.W. Gymer, A.B. Holmes, J.H. Burroughes, R.N. Marks, C. Taliani, D.D.C. Bradley, D.A.D. Santos, J.L. Brédas, M. Lögdlund, W.R. Salaneck, Electroluminescence in conjugated polymers, Nature, 397, 121-128 (1999).
3. J. Stejskal, P. Kratochvíl, A.D. Jenkins, The formation of polyaniline and the nature of its structures, Polymer, 37, 367-369 (1996).
4. N.E. Agbor, M.C. Petty, A.P. Monkman. Polyaniline thin films for gas sensing. Sens. Act., B28, 173-179 (1995).
5. S. Karg, J.C. Scott, J.R. Salem, M. Angdopoulos, Increased brightness and lifetime of polymer light-emitting diodes with polyaniline anodes, Synth. Met., 30 (1996) 111-117.
6. A. Talo, P. Passiniemi, O. Forsén, S. Yläsaari, Polyaniline/epoxy coatings with good anti-corrosion properties, Synth. Met., 85, 1333-1334, (1997).
7. Y. Xi, J.M. Wiesinger, A.G. MacDiarmid, A.J. Epstein, Camphorsulfonic acid fully doped polyaniline emeraldine salt: conformations in different solvents studied by an ultraviolet/visible/near-infrared spectroscopic method. Chem. Mater, 7, 443-445 (1995).
8. Y. Ma, N. Li, C. Yang, X. Yang, One-step synthesis of water-soluble gold nanoparticles/polyaniline composite and its application in glucose sensing, Colloids and Surfaces A: Physicochem. Eng. Aspects, 269, 1-6 (2005).
9. K. Nakajima, K. Kawabata, H. Goto, Water soluble polyaniline/polysaccharide composite: polymerization, carbonization to yield carbon micro-bubbles. Synth. Met., 194, 47-51 (2014).
10. Z. Zhang, M. Wan, Composite films of nanostructured polyaniline with poly(vinyl alcohol). Synth. Met., 128, 83-89 (2002).
11. M.S. Cho, S.Y. Park, J.Y. Hwang, H.J. Choi, Synthesis and electrical properties of polymer composites with polyaniline nanoparticles, Mater. Sci. Eng. C. 24, 15-18 (2004).
12. M. Yang, B. Cheng, H. Song, X. Chen, Preparation and electrochemical performance of polyaniline-based carbon nanotubes as electrode material for supercapacitor, Electrochimica Acta, 55, 7021–7027 (2010).
13. Y. Gu, J. Huang, Nanographite sheets derived from polyaniline nanocoating of cellulose nanofibers, Mater. Res. Bull., 48, 429-434 (2013).
14. K. Abe, S. Iwamoto, H. Yano, Obtaining Cellulose nanofibers with a uniform width of 15 nm from wood, Biomacromolecules, 8, 3276-3278 (2007).
15. A. Isogai, T. Saito, H. Fukuzumi, TEMPO-Oxidized cellulose nanofibers, nanoscale, 3, 71-85, (2011).
16. S. Iwamoto, K. Abe, H. Yano, The effect of hemicelluloses on wood pulp nanofibrillation and nanofiber network characteristics, Biomacromolecules 9, 1022-1026 (2008).
17. M. Sossna, M. Hollas, J. Schaper, T. Schaper, Structural development of asymmetric cellulose acetate microfiltration membranes prepared by a single-layer dry-casting method, J. Memb. Sci., 289, 7-14 (2007).
18. M. Nogi, H. Yano, Transparent nanocomposites based on cellulose produced by bacteria offer potential innovation in the electronics device industry, Adv. Mater., 20, 1849-1852 (2008).
19. M. Nogi, S. Iwamoto, A.N. Nakagaito, H. Yano, Optically transparent nanofiber paper, Adv. Mater., 21, 1595-1598 (2009).
20. H. Yano, J. Sugiyama, A.N. Nakagaito, M. Nogi, T. Matsuura, M. Hikita, K. Handa, Optically transparent composites reinforces with networks of bacterial nanofibers, Adv. Mater.,17, 153-155 (2005).
21. S. Iwamoto, A.N. Nakagaito, H. Yano, M. Nogi, Optically Transparent composites reinforced with plant fiber-based nanofibers, Appl. Phys. A81, 1109-1112 (2005).
22. H. Peng, G. Ma, W. Ying, A. Wang, H. Huang, Z. Lei, In Situ synthesis of polyaniline/sodium carboxymethyl cellulose nanorods for high-performance redox supercapacitors. J. Power Sources, 21, 40-45 (2012).
23. J.A. Marins, B.G. Soares, K. Dahmouche, S.J.L. Ribeiro, H. Barud, D. Bonemer, Structure and properties of conducting bacterial cellulose-polyaniline nanocomposites, Cellulose, 18, 1285-1294 (2011).

24. H. Wang, E. Zhu, J. Yang, P. Zhou, D. Sun, W. Tang, Bacterial cellulose nanofiber-supported polyaniline nanocomposites with flake-shaped morphology as supercapacitor electrodes, J. Phys. Chem. C, 116, 13013-13019 (2012).
25. M. Wan, Absorption spectra of thin film of polyaniline, J. Polym. Sci. A. Polym. Chem, 30, 543-549 (1992).
26. A.A. Qaiser, M.M. Hyland, D.A. Patterson, Surface and charge transport characterization of polyaniline−cellulose acetate composite membranes, J. Phys. Chem. B, 113, 1652-1661 (2011).
27. P.K. Kahol, N.J. Pinto, Electron paramagnetic resonance investigations of electrospun polyaniline fibers, Solid State Commun, 124, 195-197 (2002).
28. S.M. Yang, K.H. Chen, Y.F. Yang, Synthesis of polyaniline nanotubes in the channels of anodic alumina membrane, Synth. Met., 152, 65-68 (2005).
29. A.G. MacDiarmid, A.J. Epstein, Secondary doping in polyaniline, Synth. Met, 69, 85-92 (1995).